Laminar-Flow Fluid Mixer for Fast Fluorescence Kinetics Studies

Suzette A. Pabit and Stephen J. Hagen
Department of Physics, University of Florida, Gainesville, Florida 32611 USA

ABSTRACT The ability to mix aqueous liquids on microsecond time scales, while consuming minimal amounts of sample and maintaining UV-visible optical access to the mixing region, is highly desirable for a range of biophysical studies of fast protein and nucleic acid interactions and folding. We have constructed a laminar coaxial jet mixer that allows the measurement of UV-excited fluorescence from nanoliter and microliter quantities of material, mixed at microsecond rates. The mixer injects a narrow cylindrical stream (radius $a < 1$ μm) of fluorescent sample into a larger flow of diluting buffer that moves through a capillary (100 μm i.d.) at a speed ~20 cm/s, under laminar flow conditions ($Re \approx 14$). Construction from a fused silica capillary allows the laser excitation (at 266 nm) and detection (at 350 nm) of tryptophan fluorescence at reasonably low working concentrations, without interference from background fluorescence. Using this mixer we have measured submillisecond fluorescence quenching kinetics while consuming fluorescent sample at rates no greater than 6 nl/s. Consumption of the diluting buffer is also very modest (~1–3 μl/s) in comparison with other rapid mixer designs.

INTRODUCTION

New experimental techniques for triggering and probing fast conformational dynamics and folding in proteins and nucleic acids, on time scales of nanoseconds and microseconds, have significantly advanced our understanding of these important biophysical phenomena (Callender et al., 1998; Eaton et al., 2000). Some of the advances with greatest impact include the development of laser-based photochemical triggers for folding, the development of laser temperature-jump spectrometers, and the construction of ultrarapid fluid-mixing devices (Roder and Shastry, 1999). Although laser-based photochemical and *T*-jump techniques will always offer superior time resolution in kinetics studies, ultrarapid mixers, which combine two fluids at microsecond rates for spectroscopic investigation of the product, offer an important advantage: a fast solvent change can generate a large thermodynamic perturbation on virtually any biomolecular system. Thus, the continued improvement of rapid mixing technologies remains an important avenue toward progress in the study of protein and nucleic acid interactions and folding.

The mixing of two fluids ultimately relies on molecular diffusion to generate a uniform spatial distribution in solute concentrations. Because time scales for diffusion vary as the square of the distance over which solutes must diffuse, rapid mixing is possible only if the length scales of the initial heterogeneity are very short (Brody et al., 1996). For example, sub-millisecond mixing of typical small molecule solutes with diffusion constants $D \approx 10^{-5}$ cm^2/s requires that this length scale cannot exceed $[Dt]^{1/2} \approx 1$ μm. Turbulent flows can significantly accelerate mixing, because the action of eddies can premix the solutions down to these microscopic length scales (Regenfuss et al., 1985). One approach to achieving microsecond mixing times is therefore to generate turbulent flow within the mixer, i.e., to drive the flow at a high Reynolds number. The dimensionless Reynolds number is $Re = \rho v d/\eta$, where ρ is the fluid density, η is the dynamic viscosity, v is the fluid velocity, and d is the characteristic spatial dimension, such as the diameter of the flow channel (Constantinescu, 1995). Although effective for mixing, this approach tends to yield poor sample economy: if the sample consumption Q (volume/time) scales as $Q \approx \pi v d^2/4 \approx Re d\eta/\rho$, one expects all but the smallest turbulent mixers to consume large amounts of sample. Thus, although some turbulent mixers have achieved impressive mixing dead times of ~100 μs or better, these consume sample rapidly, typically ~0.5–2 ml/s (Moskowitz and Bowman, 1966; Takahashi et al., 1995; Chan et al., 1997; Shastry et al., 1998; Bökenkamp et al., 1998). Protein consumption in ultrarapid mixing studies has been as high as 8 mg/s (Akiyama et al., 2002). Folding kinetics of poorly expressed (or otherwise scarce) proteins would be difficult to study under such conditions. Furthermore, the scaling of Q with Re suggests that reducing sample consumption to a level of ~1 ml/min, while still maintaining turbulent flow in a cylindrical channel (i.e., $Re \approx 2 \times 10^3$), would require a channel diameter of order $d \approx 10$ μm and a flow speed $v \approx 210$ m/s. Given the practical difficulties likely to arise with such a device, alternatives to turbulent mixing have begun to attract attention.

Mixing can be rapid under laminar flow conditions (low Re), if the mixer is designed to draw the two solutions into sufficiently thin parallel layers. Knight and coworkers (1998) used lithographic techniques to fabricate a laminar mixer with micron dimensions. They used a rectangular, hydrodynamic-focusing geometry, in which a thin sheet of sample is pinched between two layers of diluting buffer; solute diffuses into the sheet in a largely one-dimensional manner. Pollack and coworkers subsequently used this de-

Submitted April 26, 2002, and accepted for publication June 27, 2002.

Address reprint requests to Dr. Stephen J. Hagen, Department of Physics, University of Florida, P.O. Box 118440, Gainesville, FL 32611-8440; Tel.: 352-392-4716; Fax: 352-392-7709; E-mail: sjhagen@ufl.edu.

0006-3495/02/11/2872/07 $2.00

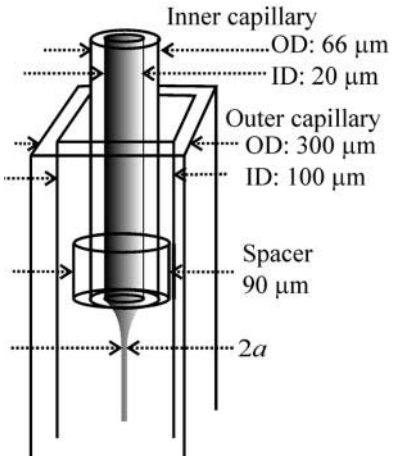

FIGURE 1 Schematic of the laminar coaxial mixer. A stream of fluorescent sample exiting the inner capillary is entrained in a flow of diluting buffer passing through the outer capillary. This draws the sample stream into a column of radius $a \approx 1$ μm, allowing rapid diffusional exchange of solute ions with the surrounding buffer. The use of fused silica capillary provides UV transparency.

sign in x-ray scattering investigations of protein and RNA folding dynamics (Pollack et al., 1999; Russell et al., 2002), obtaining a time resolution on order of ~350 μs. However, because the mixer materials are not UV-transparent, the Knight et al. design is not easily adapted to kinetic studies that probe the excitation (at 260–290 nm) and emission (~ 350 nm) of tryptophan fluorescence. Because tryptophan fluorescence is a standard biophysical probe in bench-top-level studies of protein folding dynamics, we have sought to develop a sample-efficient device that mixes fluids with microsecond dead times under laminar flow conditions, while at the same time allowing broad UV-visible optical access to the sample.

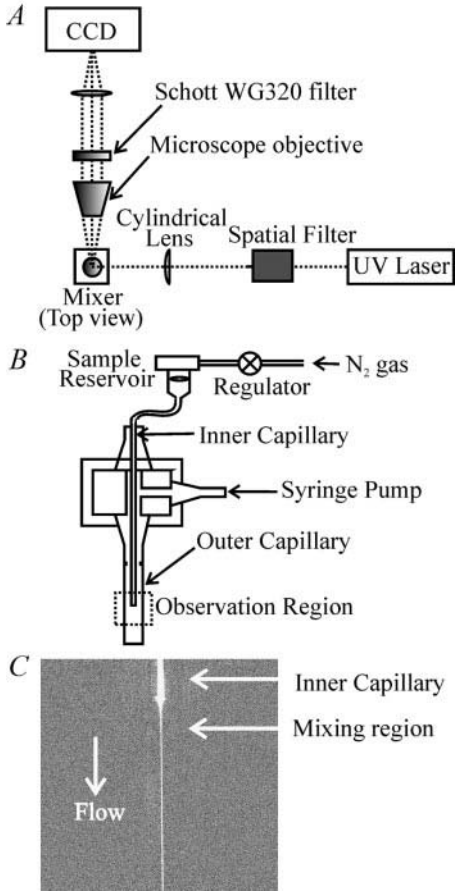

FIGURE 2 (*A*) Schematic of fluorescence excitation and collection optics: the flowing sample is illuminated by an UV laser and imaged onto a CCD. (*B*) Sample delivery system, consisting of a N_2 pressure regulator for driving inner-capillary flow and a programmable syringe pump for controlling flow of diluting buffer in the outer capillary. Tubing connections are made with Luer fittings and microbore tubing (500 μm i.d.). (*C*) Background-subtracted CCD image of a fluorescent dye passing through the mixer. The hyrodynamic focusing by the outer capillary buffer is evident.

MATERIALS AND METHODS

Mixer design and operation

We have constructed a coaxial laminar jet mixer that satisfies these requirements (Fig. 1). A fluorescent sample (e.g., protein) flows out of a narrow capillary and is released into the center of a flow of diluting buffer that passes through a larger outer capillary. The resulting fluorescent stream is hydrodynamically focused to a narrow cross section as it is accelerated by the outer capillary flow. As the inner stream is thus drawn out into a thin column, radial diffusion of solute ions between the sample and the diluting buffer can occur rapidly, providing fast mixing. The device is constructed from narrow fused silica capillary of 20 μm i.d. and 66 μm o.d. (Polymicro Technologies, Phoenix, AZ), which is inserted into a second silica capillary. The outer capillary has square cross section, with an inside width of 100 μm. The cylindrical inner capillary carries a thin outer coating of polyimide (90 μm o.d.) that acts as a spacer, keeping the inner and outer capillaries concentric. Using laser illumination and a CCD detector, we have measured fluorescence quenching reaction kinetics occurring at microsecond rates in the fluorescent stream. For typical parameters of ~5 ml/h flow rate in the outer capillary (for an axial flow velocity of ~22 cm/s), the mixer consumes 1.4 μl/s of the diluting buffer and 0.2–6 nl/s of fluorescent sample. CCD exposure times of 10–45 s are sufficient for measuring quenching rates. The flow pattern, which is characterized by $Re \approx 14$, is stable and time independent.

The mixer operates in continuous flow. The fluorescence of the mixing stream is imaged onto a CCD array, and the spatial position of a point in the flow is a linear function of the time elapsed since mixing. The fluorescent stream does not diffuse far from the central axis of the flow before passing out of the mixer. Although the flow remains confined within the mixer at all times, the use of the fused silica capillary makes the entire mixing and reaction region UV-transparent (Fig. 2 *A*). We focus the 266-nm fourth harmonic of a quasi-CW Nd:YAG laser (2 mW, NanoUV, JDS Uniphase, San Jose, CA) through a cylindrical lens and onto the mixer to excite tryptophan fluorescence in the sample stream. A 10× long-working-distance microscope objective, 0.3 N.A., ∞-corrected (Olympus America, Melville, NY) collects the 350-nm emission, which passes through a Schott WG-320 filter and silica tube lens before being imaged onto a UV-sensitive 1300 × 1030 pixel CCD (Micromax, Roper Scientific, Princeton, NJ). The 6.7-μm × 6.7-μm pixel size of the CCD therefore implies a nominal time resolution of 3.4 μs at a flow speed of 20 cm/s, although our actual resolution is reduced by binning of the pixels. A

background image is subtracted from all fluorescence images. Mixing data presented here were obtained at 22°C.

The coaxial mixer is assembled under a microscope and held in a machined sample holder with Luer connections (Fig. 2 *B*). A programmable syringe pump supplies a fixed flow of buffer through the outer capillary. The much smaller flow rates through the inner capillary are maintained by gas pressure (~5–25 psi N_2) controlled by a precision regulator (Omega Engineering, Meriden, CT). Fig. 2 *C* shows a typical fluorescence image of the operating mixer. Because of the nonuniform velocity profile of a viscous fluid flowing through a rectangular channel, the fluid velocity along the central axis of the outer capillary exceeds the cross-sectional average flow velocity set by the syringe pump (Constantinescu, 1995; Brody et al., 1996). For a square capillary, the ratio of the maximum speed at the center of the capillary to the average speed is ~1.6. We use this central axis velocity, rather than the average velocity, as the scale factor to convert spatial fluorescence data (from the CCD) into time-dependent fluorescence decay data.

This design represents a microfluidic analog of the larger coaxial jet mixer described by Christian and coworkers for flow cytometry applications (Scampavia et al., 1995; Andreev et al., 1999). That device mixes two concentric streams of liquid throughout the volume of the cylindrical observation channel, rather than just along the central axis (as in our mixer). Therefore, when operating under laminar conditions, the larger mixer required diffusion across the relatively wide (hundreds of microns) channel, generating mixing times of ~10 s with sample consumption of 60 μl/min. Under turbulent flow conditions, those authors obtained a dead time of ~55 ms (Scampavia et al., 1995). Our design reduces the physical dimensions and confines the mixing region to the central axis of the flow, which generates at least a 100-fold improvement in dead time (to ~400 μs; see below), and at least a 160-fold reduction in sample consumption, while maintaining laminar flow.

Modeled behavior

The particularly simple cylindrical geometry allows us to model the behavior of the mixer with a radial diffusion equation:

$$\frac{\partial C(r,t)}{\partial t} = \frac{D}{r}\left(\frac{\partial C}{\partial r} + r\frac{\partial^2 C}{\partial r^2}\right) \quad (1)$$

We consider a quenching experiment, where the outer capillary buffer contains a high initial concentration C_0 of a diffusing solute that quenches fluorescence of the inner capillary sample. Then $C(r, t)$ is the concentration of the outer capillary solute at radius r (distance from the mixer axis) and time t, and D is the solute diffusion constant. Fig. 3 *A* shows concentration profiles $C(r, t)$ obtained by numerical solution of Eq. 1, with the initial condition that $C(r, 0) = 0$ for $r < a$ and $C(r, 0) = C_0$ for $r > a$, and a is the radius of the inner capillary stream. The concentration at $r = 0$ rises from $C = 0$ to $C \approx (0.5)C_0$ in a time $t \approx a^2/3D$, and to $C \approx (0.9)C_0$ in a time $t \approx 2a^2/D$. Fig. 3 *B* shows the time dependence of the rising concentration at $r = 0$ in more detail. The figure allows an interesting comparison between two geometries for fast laminar mixing, i.e., between radial diffusion in the coaxial mixer and one-dimensional diffusion in the flat-sheet mixer of Knight et al. (1998). Even though both curves assume a similar length scale for diffusion, the rise time (to 90% of C_0) for the concentration at $r = 0$ is ~20 times faster in the coaxial geometry than in the rectangular geometry: cylindrical diffusion is more abrupt, and experiments requiring a well defined final solute concentration C_0 would tend to benefit from this geometry. The hydrodynamics of the coaxial design are also simpler in principle, because the fluorescent stream remains in the center of the channel and avoids the stationary boundary layer at the walls.

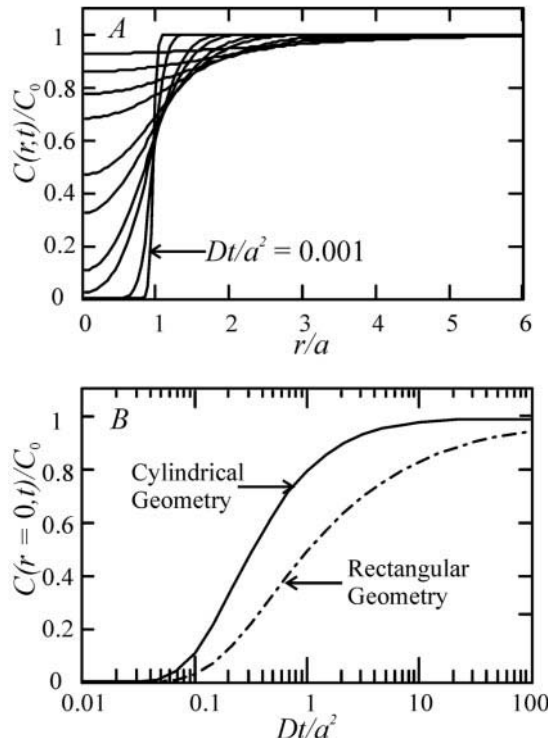

FIGURE 3 (*A*) Numerical solutions to the cylindrical diffusion equation (Eq. 1) for diffusion of a solute from a diluting buffer (initial concentration C_0) into a sample stream of radius a, with initial concentration $C(r < a, t = 0) = 0$. The curves represent the concentration profiles at dimensionless times $Dt/a^2 = 0.001$, 0.01, 0.06, 0.1, 0.2, 0.3, 0.6, 0.9, 1.5, and 3. (*B*) Comparison of laminar mixing in cylindrical versus rectangular geometries: the solid line describes radial diffusion of solute into a cylindrical stream of diameter $2a$, whereas the broken line describes one-dimensional diffusion (from both sides) into a flat sheet of thickness $2a$. Curves were obtained from numerical solution of diffusion equations and show solute concentration at the center of the cylinder or sheet.

RESULTS

Mixer performance

Quantitative fluorescence measurement

Fig. 4 demonstrates a quantitative fluorescence measurement in the mixer. The inner capillary contains 50 μM of the fluorophore, *N*-acetyl-tryptophanamide (NATA) in 100 mM phosphate buffer (pH 7), whereas the outer capillary contains 34 mM sodium iodide. Mixing of these solutions results in quenching of the tryptophan fluorescence by the iodide ion in a diffusion-limited reaction, with a bimolecular rate of $\sim 4 \times 10^9$ $(M\ s)^{-1}$ (Lehrer, 1971). The Stern Volmer plot from an equilibrium study (Fig. 4 *D*) shows that 34 mM is the midpoint concentration $C_{1/2}$, at which the NATA fluorescence should be reduced twofold. A CCD image of NATA-NaI mixing was collected at a constant outer capillary flow rate and constant inner capillary driving pressure. Immediately afterwards, a background image was collected by suppressing flow in the inner capillary while

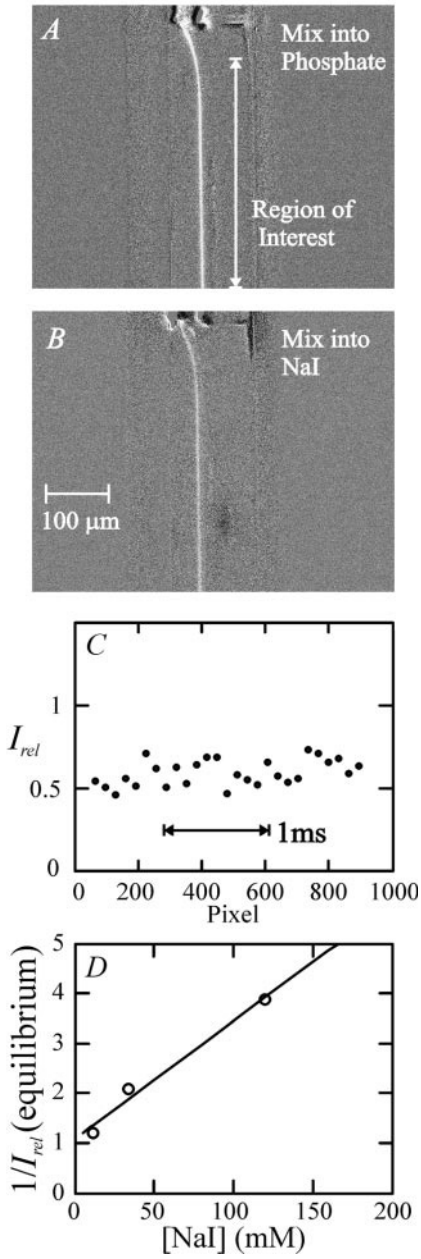

FIGURE 4 Quantitative fluorescence measurement in the coaxial mixer. (*A*) Image of control experiment in which NATA flowing from the inner capillary mixes with (inert) phosphate, pH 7, in the outer capillary. Driving pressure for the inner capillary flow is 6 psi and outer capillary flow rate is 5 ml/h. Background has been subtracted from the image. (*B*) Image of quenching experiment in which NATA mixes with 34 mM NaI flowing in the outer capillary, under the same flow conditions as above. (*C*) Intensity ratio $I_{rel} = I_{reaction}/I_{control}$ calculated from above images, as a function of distance downstream from point of mixing (in pixels). The figure indicates $I_{rel} \approx 50\%$, as expected from equilibrium data of *D*. (*D*) Stern-Volmer plot of the NATA-NaI quenching reaction, from equilibrium fluorimetry.

allowing the outer capillary flow to continue. The images were subtracted in the CCD data acquisition software (WinView, Roper Scientific, Princeton, NJ). A control experiment was then performed by mixing NATA into phosphate buffer (iodide-free) under the same flow conditions. Fig. 4, *A* and *B*, show the resulting background-subtracted images. After image data were transferred to MATLAB (Mathworks, Natick, MA), the pixels downstream of the mixing region were binned along the vertical spatial direction (time axis), and a relative fluorescence ($I_{rel} = I_{reaction}/I_{control}$) was calculated for each binned time. Fig. 4 *C* indicates that $I_{rel} \approx 0.5$, giving quantitative agreement with the equilibrium fluorescence data.

Measurement of reaction rates

The time-resolution of mixers is best measured with a standard chemical-kinetic reaction, the quenching of NATA fluorescence by *N*-bromosuccinimide (NBS). This proceeds at a bimolecular rate $k_{bi} \approx (7.3–7.9) \times 10^5\ (\mathrm{M\ s})^{-1}$ at room temperature (Peterman, 1979; Shastry et al., 1998). Fig. 5 shows a mixing experiment in which 50 μM NATA flows in the inner capillary and 1.5 mM NBS flows in the outer capillary, under several different driving pressures for the inner capillary. The outer capillary flow rate remains fixed at 5 ml/h. The quenching reaction at these concentrations should progress with pseudo-first-order kinetics at a rate $k_0 \approx [\mathrm{NBS}]\ k_{bi} = 1100–1200\ \mathrm{s}^{-1}$.

The intensity plots in Fig. 5, *B*—*D*, show exponential decay of I_{rel} as a function of distance downstream from the point of mixing. From the decay rate s (units of pixels^{-1}) obtained in an exponential fit, the distance $\delta x = 0.67\ \mu$m imaged by one pixel, and the stream axial velocity v, we obtain the apparent quenching rate $k = sv/\delta x$ (with units of s^{-1}). This rate tends to increase as the driving pressure P_{inner} on the sample reservoir is reduced, a behavior that is anticipated as a consequence of laminar mixing: lower pressures in the inner capillary drive a smaller volume of fluorescent material into the mixer, resulting in a narrower fluorescent stream, faster molecular diffusion, and more rapid quenching of the fluorescence. High pressures, by contrast, result in a broader stream of NATA, which slows the diffusion of NBS and delays the quenching reaction. Thus the observed quenching rate at high pressure is controlled by the speed of molecular diffusion, whereas in the limit of very low pressures we expect the intrinsic reaction rate k_0 to control the apparent quenching rate. Fig. 6 *A* demonstrates that this is indeed the case. As the driving pressure decreases toward 5 psi, k approaches k_0, and the observed fluorescence decay provides an accurate measurement of the submillisecond reaction rate.

Fig. 6 *B* shows that the total fluorescence intensity of the stream grows linearly with driving pressure P_{inner} when an inert buffer is used in the outer capillary. This indicates that the cross-sectional area of the fluorescent stream grows in proportion to P_{inner}, and it reflects the fact that the volume flow rate Q in the stream equals that delivered by the cylindrical inner capillary (of length L and inner radius R). One expects the capillary flow rate to be proportional to the

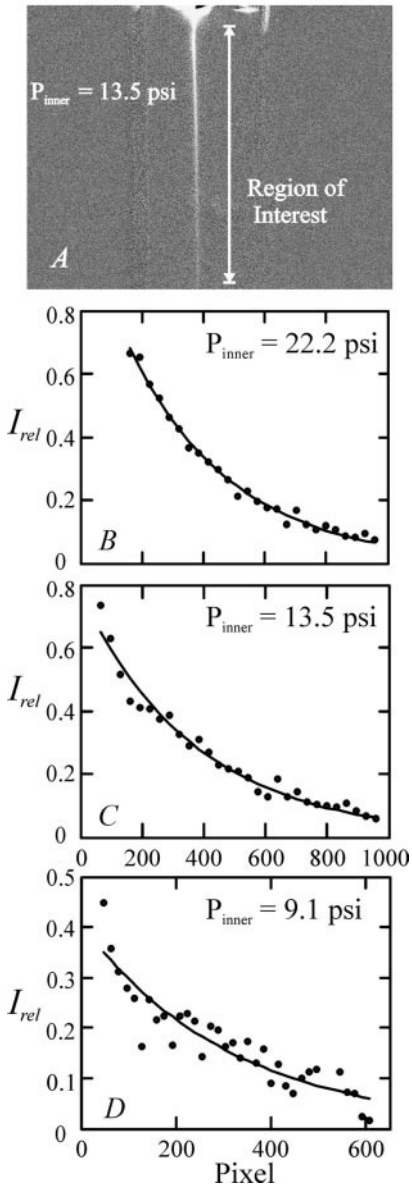

FIGURE 5 Kinetics of NATA-NBS quenching reaction studied in coaxial mixer. (*A*) Typical image of NATA (50 μM) flowing from the inner capillary (at 13.5 psi driving pressure) and mixing with 1.5 mM NBS in the outer capillary (at 5 ml/h). The NATA fluorescence decays with distance ($\propto$ time) downstream from the point of mixing, owing to a bimolecular quenching reaction with NBS ($k_{bi} = (7.3–7.9) \times 10^5\ M^{-1}\ s^{-1}$). The figure also shows relative fluorescence I_{rel} as a function of position for different inner capillary pressures: 22.2 psi (*B*), 13.5 psi (*C*), and 9.1 psi (*D*). The decay rate *s* obtained from exponential fits to I_{rel} (*solid lines*) is related to the apparent quenching rate *k* by $k = sv/\delta x$, where $v = 22$ cm/s is the velocity of the fluorescent stream and $\delta x = 0.67$ μm is the size of the region imaged by one CCD pixel.

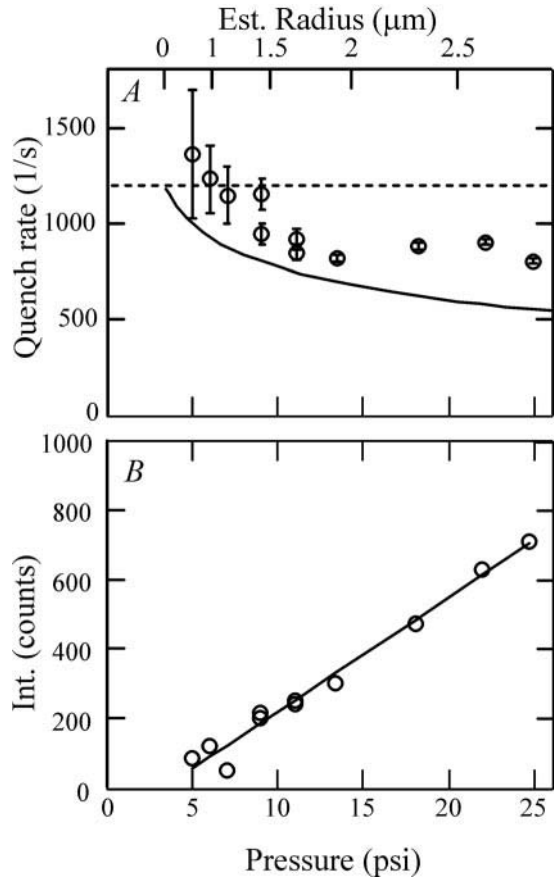

FIGURE 6 (*A*) Variation of the apparent rate of fluorescence quenching of NATA (50 μM) by NBS (1.5 mM) with inner-capillary driving pressure (○). Lower driving pressures reduce the volume of flow, shrinking the radius of the NATA stream and allowing faster diffusion of NBS. The apparent quenching rate then approaches the expected value for this bimolecular reaction (---). At higher pressures, the fluorescent stream widens and the quenching rate becomes diffusion controlled. The solid curve is the behavior predicted by a numerical model of Eqs. 1 and 2. (*B*) The overall fluorescence intensity of the inner stream (in a nonquenching buffer) versus inner-capillary driving pressure. Intensity grows linearly with pressure, because flow volume is proportional to the driving pressure gradient (Eq. 2). The flow cuts off when the driving pressure equals the pressure $P_0 = 3.5$ psi in the outer capillary at the point of mixing.

driving pressure gradient (Hagen, 1839; Poiseuille, 1840, 1841; Constantinescu, 1995):

$$Q = \frac{\pi R^4}{8\eta}\frac{\partial P}{\partial z} \qquad (2)$$

where η is the viscosity of the sample and $\partial P/\partial z = (P_{inner} - P_0)/L$ is the pressure gradient between the sample reservoir (pressure P_{inner}) and the terminus of the inner capillary (pressure P_0). The intercept on Fig. 6 *B* then indicates that the pressure in the mixing region is $P_0 \approx 3.5$ psi. From the parameters of the inner capillary ($L \approx 105$ mm; $R \approx 10$ μm), and $\eta \approx 0.01$ P, we can use Eq. 2 to estimate $Q = 0.3$ nl/s at our lowest pressures ($P_{inner} \approx 5$ psi), and from the axial flow speed $v = 21$ cm/s we estimate the stream radius $a = (Q/\pi v)^{1/2} \approx 0.7$ μm at these pressures. Reaction rates up to $3D/a^2 \approx 3000\ s^{-1}$ should be measurable under these conditions if $D \approx 5 \times 10^{-6}$ cm^2/s, whereas higher rates would be accessible with lower pres-

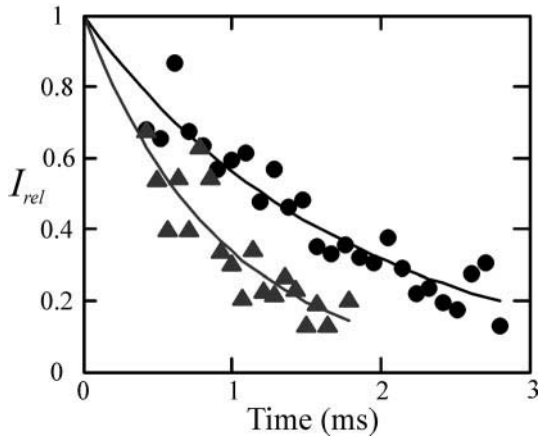

FIGURE 7 Kinetics of the fluorescence quenching reaction between NATA (at 50 μM) and NBS at 1.5 mM (▲) and 0.75 mM (●). Exponential fits (——) give first-order rates $k = 575 \pm 52\ s^{-1}$ and $1086 \pm 107\ s^{-1}$, respectively, consistent with expected values of 540–590 s^{-1} and 1100–1200 s^{-1}. Backward extrapolation of the fits to $I_{rel} = 1$ provides an estimate of the mixing dead time, $t_{dead} \approx 425\ \mu s$.

sures or with faster diffusing species (such as H^+ in a pH jump).

Taking advantage of the simple physics of Eqs. 1 and 2, we constructed a numerical model of the mixer in MATLAB. The model solves Eqs. 1 and 2 for the generation of the sample stream of NATA, with the simultaneous inward diffusion and reaction of NBS, to predict the apparent rate of fluorescence quenching. The predicted behavior (solid line in Fig. 6 *A*) closely resembles the actual data, although there is some deviation at high driving pressures. The curve shown assumes a diffusion constant $D = 7 \times 10^{-6}\ cm^2/s$ for NBS and a pressure $P_0 = 3.5$ psi in the mixing region (as suggested by Fig. 6 *B*) but has no free parameters. The deviation between data and model may arise from the outward diffusion of the NATA away from the central axis, an effect (not included in the model) that would tend to enhance the apparent quenching rate under diffusion-limited conditions. In the case of a protein folding experiment, for which the fluorescent protein diffuses more slowly than the solute ions, we would expect the actual performance to match the modeled curve more closely.

Dead time of mixing

The mixing dead time, t_{dead}, is the elapsed time between the initiation of mixing and the first observable point where mixing is complete (Peterman, 1979). If the relative fluorescence data of Fig. 6 are extrapolated backwards to the point where $I_{rel} = 1$, and that point is defined as $t = 0$, then the first observable point in the fluorescence decay curve occurs at t_{dead}. Fig. 7 shows this extrapolation for two measurements of the quenching of 50 μM NATA by 0.75 mM and 1.5 mM NBS, in the fast (i.e., low P_{inner}) limit of mixer operation. The fluorescence decays indicate quenching rates of $575 \pm 52\ s^{-1}$ and $1086 \pm 107\ s^{-1}$, respectively, in satisfactory agreement with the expected values 540–590 s^{-1} and 1100–1200 s^{-1}. Furthermore, the figure indicates $t_{dead} \approx 425\ \mu s$. Because each measurement consumed less than $\sim 1\ \mu l$ of 50 μM NATA, the figure shows that quantitative UV-fluorescence studies of microsecond reactions can be performed while using only picomole quantities of material.

We expect that geometrical parameters define the dead time of this mixing device. The flow dynamics and diffusional transport near the terminus of the inner capillary are nonuniform and quite complex, because the fluorescent stream broadens as it exits the inner capillary and then narrows as it is accelerated by the faster flow of surrounding buffer. This region thus represents an effectively dead volume for the mixer. However, the flow leaves this region and should attain its steady-state flow profile over an entry length $x \approx 0.05 dRe = 0.05\ \rho v d^2/\eta \approx 75\ \mu m$ (Constantinescu, 1995), where $d = 100\ \mu m$ is the width of the outer capillary and $v = 14$ cm/s is the (typical) mean flow speed. This suggests that the mixing dead time will be $x/v \approx 0.05\ \rho d^2/\eta \approx 500\ \mu s$, independent of flow speed. This estimate is consistent with the data of Fig. 7; moreover, the factor d^2 indicates that further reducing the dimension of the outer capillary not only is a route to improving sample efficiency, but also could substantially reduce the dead time. Because silica capillary tubing is commercially available over a wide range of sizes, significant improvement in mixer performance may be attainable without use of lithographic techniques.

CONCLUSIONS

The fabrication and continuing improvement of ultrafast fluid mixing devices is one of the driving forces behind progress in the understanding of conformational dynamics and folding of proteins and nucleic acids. Laminar (low *Re*) mixing represents an important new direction for mixing technologies, because it can lead to sub-millisecond dead times together with microliter or nanoliter sample consumption. Here we have shown that a laminar coaxial jet is a particularly simple mixing geometry that provides ready access to microsecond chemical kinetic rates through UV fluorescence spectroscopy. The method provides sufficient signal-to-noise ratio to measure fast fluorescence decays with $\sim 400\ \mu s$ dead time, while consuming only picomoles of material.

We gratefully acknowledge funding support from the National Science Foundation, MCB award 0077907, and the National Institutes of Health, NIAID award 5R01AI049063–02.

REFERENCES

Akiyama, S., S. Takahashi, T. Kimura, K. Ishimori, I. Morishima, Y. Nishikawa, and T. Fujisawa. 2002. Conformational landscape of cytochrome *c* folding studied by microsecond-resolved small-angle x-ray scattering. *Proc. Natl. Acad. Sci. U.S.A.* 99:1329–1334.

Andreev, V. P., S. B. Koleshko, D. A. Holman, L. D. Scampavia, and G. D. Christian. 1999. Hydrodynamics and mass transfer of the coaxial jet mixer in flow injection analysis. *Anal. Chem.* 71:2199–2204.

Bökenkamp, D., A. Desai, X. Yang, Y.-C. Tai, E. M. Marzluff, and S. L. Mayo. 1998. Microfabricated silicon mixers for submillisecond quench-flow analysis. *Anal. Chem.* 70:232–236.

Brody, J. P., P. Yager, R. E. Goldstein, and R. H. Austin. 1996. Biotechnology at low Reynolds number. *Biophys. J.* 71:3430–3441.

Callender, R. H., R. B. Dyer, R. Gilmanshin, and W. H. Woodruff. 1998. Fast events in protein folding: the time evolution of primary processes. *Annu. Rev. Phys. Chem.* 49:173–202.

Chan, K., Y. Hu, S. Takahashi, D. Rousseau, and W. Eaton. 1997. Submillisecond protein folding kinetics studied by ultrarapid mixing. *Proc. Natl. Acad. Sci. U.S.A.* 94:1779–1784.

Constantinescu, V. N. 1995. Laminar Viscous Flow. Springer-Verlag, New York.

Eaton, W. A., V. Muñoz, S. J. Hagen, G. S. Jas, L. Lapidus, E. R. Henry, and J. Hofrichter. 2000. Fast kinetics and mechanisms in protein folding. *Annu. Rev. Biophys. Biomol. Struct.* 29:327–359.

Hagen, G. 1839. Ueber die Bewegung des Wassers in engen cylidrischen Rohren. *Poggendorfs Ann. Phys. Chem.* 46:423–442.

Knight, J. B., A. Vishwanath, J. P. Brody, and R. H. Austin. 1998. Hydrodynamic focusing on a silicon chip: mixing nanoliters in microseconds. *Phys. Rev. Lett.* 80:3863–3866.

Lehrer, S. S. 1971. Solute perturbation of protein fluorescence: the quenching of the trytophyl fluorescence of model compounds and lysozyme by iodide ion. *Biochemistry.* 10:3254–3263.

Moskowitz, G. W., and R. L. Bowman. 1966. Multicapillary mixer of solutions. *Science.* 153:428–429.

Peterman, B. F. 1979. Measurement of the dead time of a fluorescence stopped-flow instrument. *Anal. Biochem.* 93:442–444.

Pollack, L., M. W. Tate, N. C. Darnton, J. B. Knight, S. M. Gruner, W. A. Eaton, and R. H. Austin. 1999. Compactness of the denatured state of a fast-folding protein measured by submillisecond small-angle scattering. *Proc. Natl. Acad. Sci. U.S.A.* 96:10115–10117.

Poiseuille, J. L. M. 1840/1841. Recherches expérimentales sur le mouvement des liquides dans les tubes de très-petits diamètres. *CR Acad. Sci. Paris.* 11:961–967, 1041–1049/12:112–115.

Regenfuss, P., R. M. Clegg, M. J. Fulwyler, F. J. Barrantes, and T. M. Jovin. 1985. Mixing liquids in microseconds. *Rev. Sci. Instr.* 56: 283–290.

Roder, H., and M. C. R. Shastry. 1999. Methods for exploring early events in protein folding. *Curr. Opin. Struct. Biol.* 9:620–626.

Russell, R., I. S. Millett, M. W. Tate, L. W. Kwok, B. Nakatani, S. M. Gruner, S. G. J. Mochrie, V. Pande, S. Doniach, D. Herschlag, and L. Pollack. 2002. Rapid compaction during RNA folding. *Proc. Natl. Acad. Sci. U.S.A.* 99:4266–4271.

Scampavia, L. D., G. Blankenstein, J. Ruzicka, and G. D. Christian. 1995. A coaxial jet mixer for rapid kinetic analysis of flow injection and flow injection cytometry. *Anal. Chem.* 67:2743–2749.

Shastry, M. C. R., S. D. Luck, and H. Roder. 1998. A continuous-flow capillary mixing method to monitor reactions on the microsecond time scale. *Biophys. J.* 74:2714–2721.

Takahashi, S., Y.-C. Ching, J. Wang, and D. L. Rousseau. 1995. Microsecond generation of oxygen-bound cytochrome *c* oxidase by rapid solution mixing. *J. Biol. Chem.* 270:8405–8407.